Glia

WILEY

GLIA

RESEARCH ARTICLE OPEN ACCESS

Temporal Profiling of Male Cortical Astrocyte Transcription Predicts Molecular Shifts From Early Development to Aging

Xiaoran Wei[1,2] | Jiangtao Li[2,3] | Michelle L. Olsen[2]

[1]Biomedical and Veterinary Sciences Graduate Program, Virginia Tech, Blacksburg, Virginia, USA | [2]School of Neuroscience, Virginia Tech, Blacksburg, Virginia, USA | [3]Genetics, Bioinformatics and Computational Biology Graduate Program, Virginia Tech, Blacksburg, Virginia, USA

Correspondence: Michelle L. Olsen (molsen1@vt.edu)

Received: 3 October 2024 | **Revised:** 8 February 2025 | **Accepted:** 25 February 2025

Funding: This work was supported by National Institutes of Health (R01NS120746 to M.L.O.).

Keywords: aging | astrocyte | development | transcriptome

ABSTRACT

Astrocytes are the most abundant glial cell type in the central nervous system (CNS). Astrocytes are born during the early postnatal period in the rodent brain and mature alongside neurons, demonstrating remarkable morphological structural complexity, which is attained in the second postnatal month. Throughout this period of development and across the remainder of the lifespan, astrocytes participate in CNS homeostasis, support neuronal partners, and contribute to nearly all aspects of CNS function. In the present study, we analyzed astrocyte gene expression in the cortex of wild-type male rodents throughout their lifespan (postnatal 7 days to 18 months). A pairwise timepoint comparison of differential gene expression during early development and CNS maturation (7–60 days) revealed four unique astrocyte gene clusters, each with hundreds of genes, which demonstrate unique temporal profiles. These clusters are distinctively related to cell division, cell morphology, cellular communication, and vascular structure and regulation. A similar analysis across adulthood and in the aging brain (3 to 18 months) identified similar patterns of grouped gene expression related to cell metabolism and cell structure. Additionally, our analysis identified that during the aging process astrocytes demonstrate a bias toward shorter transcripts, with loss of longer genes related to synapse development and a significant increase in shorter transcripts related to immune regulation and the response to DNA damage. Our study highlights the critical role that astrocytes play in maintaining CNS function throughout life and reveals molecular shifts that occur during development and aging in the cortex of male mice.

1 | Introduction

In mammals, astrocytes are the most abundant glial cell type in the central nervous system (CNS) (Agulhon et al. 2008; Filous and Silver 2016; Zhou et al. 2019). Previously considered largely supportive, astrocytes are now recognized for their multifaceted functions, including maintaining neuronal health, active participation in neural activity, regulation of synaptic functioning, and influence on brain metabolism and homeostasis (Vasile et al. 2017). Importantly, these functions are developmentally regulated across the lifespan of the organism.

During development, astrocytes undergo a complex and highly regulated maturation process. Astrocyte development has been extensively studied in rodent model systems. In these models, astrocyte generation starts at embryonic day 18

Xiaoran Wei and Jiangtao Li contributed equally.

(E18) or at birth, originating from radial glial cells, the same progenitor cells that give rise to neurons (Farhy-Tselnicker and Allen 2018; Miller and Gauthier 2007; Zarei-Kheirabadi et al. 2020). Soon after birth, primary astrocyte processes radiate from the cell soma, branch out, and gradually divide into finer processes, generating a dense network of delicate terminal 'leaflet' processes (Freeman 2010). Extensive process outgrowth and elaboration continue through the third postnatal week, when extra astrocyte filopodia are pruned and astrocytes establish nonoverlapping domains (Bushong et al. 2004; Bushong et al. 2002; Farhy-Tselnicker and Allen 2018; Zarei-Kheirabadi et al. 2020). Mature astrocytes across the CNS are morphologically complex cells spanning a massive spatial domain, with each astrocyte managing five to ten neuronal cell bodies, hundreds of dendrites (Halassa et al. 2007; Ogata and Kosaka 2002), and up to 100,000 individual synapses within its individual territory (Bushong et al. 2002; Freeman 2010; Oberheim et al. 2006). Astrocytes also have specialized processes called endfeet, which completely enwrap (99%) the CNS vasculature, where they participate in local blood flow regulation (Daneman and Prat 2015) and represent a critical component of the blood–brain barrier (BBB). Notably, this complex morphology is functionally related to the most well-characterized astrocyte functions, including the uptake of the neurotransmitters glutamate and GABA, K^+ ion homeostasis, synapse organization and stabilization, and blood–brain barrier integrity (Hill et al. 2019; Iadecola and Nedergaard 2007; Khakh and Sofroniew 2015). Despite the well-characterized temporal trajectory of astrocyte morphological maturation, which coincides with neuronal maturation and synaptogenesis, little is known regarding the underlying molecular mechanisms that drive this process.

Emerging evidence has demonstrated that aging astrocytes exhibit alterations in morphology, gene expression, and function. In both aging humans and rodents, astrocyte morphological changes have been observed whereby long and thin processes become short and stubby (Jyothi et al. 2015; Kanaan et al. 2010), possibly disrupting the functional and homeostatic state of astrocytes and communication with neighboring cells. Glial fibrillary acidic protein (GFAP), a classical marker of reactive astrocytes, increases during the aging process (Boisvert et al. 2018; Clarke et al. 2018; Yang and Wang 2015). Furthermore, aging astrocytes can activate the complement system, potentially contributing to cognitive decline (Palmer and Ousman 2018), increasing the production of cytokines, accumulating oxidative stress damage (Ishii et al. 2017), and impacting cholesterol synthesis and BBB integrity. These changes in morphology are unsurprisingly associated with alterations in gene expression, which demonstrate regional specificity (Boisvert et al. 2018; Matias et al. 2019) and potentially contribute to age-related neurodegenerative diseases and cognitive decline (Brandebura et al. 2023).

Understanding the complexity of astrocyte development and aging is critical for elucidating the complexity of brain function throughout the life cycle. Although astrocyte morphological complexity has been extensively studied over the past several decades, few studies have addressed the molecular shifts that drive these morphological changes during development and aging. Previous studies have used Ribotag RNA sequencing to examine actively translated genes in astrocytes during early development (Farhy-Tselnicker et al. 2021) and aging (Boisvert et al. 2018). This approach allows for the selective analysis of actively translated mRNA, but it tends to capture highly translated genes, which may introduce bias and overlook lower abundance transcripts that could still play significant roles in cellular function. Here, we utilized a magnetic bead cell pull-down method to isolate intact cortical astrocytes acutely from wild-type (WT) male mice at five early developmental time points (P7, P14, P21, P28, and P60) and across healthy aging (3, 6, 12, and 18 months). Using bulk RNA sequencing across the healthy lifespan, we achieved the goals of (1) identifying additional astrocyte-specific genes and generating a comprehensive astrocyte transcriptome; (2) characterizing the overall changes in the astrocyte transcriptome during development and senescence, including both translated and untranslated mRNAs; and (3) analyzing in detail the key periods of astrocyte maturation and the formation of "spongy" complex morphologies (P14–P28) (Akdemir et al. 2020). Our goal was to reveal the transcriptomic changes associated with the maturation of healthy astrocytes and the impact of age-related changes in gene expression. These findings enhance our understanding of the molecular changes associated with astrocytes as they achieve their remarkable morphological complexity, undergo transcriptomic maturation and aging, establish their presence at synapses, provide general homeostatic support to neurons, and participate in the formation and maturation of the blood–brain barrier formation.

2 | Methods and Materials

2.1 | Animals

Wild-type C57BL/6 male mice were housed and bred at Virginia Polytechnic Institute and State University. All experiments performed were approved by the Virginia Polytechnic Institute and State University Animal Care and Use Committee. The animals were maintained on a reverse 12 h light/dark cycle (lights on at 10 pm, lights off at 10 am) with food and water available ad libitum. All the tissue was collected between 10 am and 2 pm. To minimize potential litter effects, animals from at least three different litters were randomly assigned to each experimental group.

2.2 | Sequential Cell Isolation

The cells were isolated as previously described (Holt et al. 2019; Holt and Olsen 2016). Briefly, the mice were anesthetized with CO_2. Whole cortices were dissected in ice-cold, 95% O_2 bubbled ACSF (120 mM NaCl, 3.0 mM KCl, 2 mM $MgCl_2$, 0.2 mM $CaCl_2$, 26.2 mM $NaHCO_3$, 11.1 mM glucose, 5.0 mM HEPES with 3 mM AP5, 3 mM CNQX), and single-cell suspensions were acquired from mouse cortex using a papain dissociation kit (Worthington Biochemical, #LK003153). The cell suspensions were incubated with Myelin+ microbeads (Miltenyi Biotech #130-096-733) and CD11b+ beads (Miltenyi Biotech #130-093-634) for 10 min to remove oligodendrocytes and microglia. For the samples collected after 3 months old, CD31+ beads (Miltenyi Biotech #130-097-418) were also added to remove endothelial cell contamination. We collected the flow-through and incubated the cells in the flow-through with FcR blocking buffer for 15 min, followed by

a 15 min incubation with ACSA-2 microbeads (Miltenyi Biotech #130-097-678) to isolate astrocytes.

2.3 | RNA Isolation and qPCR

Isolated cells were stored in TRIzol (Thermo Fisher Scientific, #15596026) (−80°C) prior to RNA isolation. RNA was isolated using the Direct-zol RNA Microprep Kit (Zymo Research, #R2060) according to the manufacturer's instructions. RNA was reverse transcribed into cDNA using iScript Reverse Transcription Supermix (Bio-Red, #1708841). Astrocyte enrichment was determined by qPCR. Here, Taqman PCR master mix (Thermo Fisher Scientific, #4444557) and TaqMan probes *Gfap* (glial fibrillary acidic protein) as a marker of astrocytes, *Itgam* (integrin alpha M chain) for microglia, *Mbp* (Myelin basic protein) for myelin, *Rbfox3* (RNA binding fox-1 homolog 3) for neurons, and *Cd31* (cluster of differentiation 3, also known as platelet endothelial cell adhesion molecule) for endothelial cells, with GAPDH serving as the housekeeping gene to test the purity of two batches with qPCR. The ddCt method was employed to determine the relative mRNA expression levels. Both qPCR results showed a good purity of the astrocyte fraction (Figure S1).

2.4 | RNA Sequencing

Total RNA was reverse transcribed into the first-strand cDNA samples using the SMART-Seq v4 Ultra Low Input RNA Kit (Takara Bio, USA; Mountain View, CA, USA). PolyA enrichment was conducted to enrich all the coding RNA. The cDNA samples were then fragmented, end-repaired, A-tailed, and ligated with adaptors. After size selection and PCR enrichment, sequencing was performed on a NovaSeq instrument (Illumina). Samples from P7 to P60 were sequenced by Novogene Co., and paired-end reads 2×150 bp sequence were generated. Samples from 3 to 18 months were sequenced by MedGenome Inc. to generate paired-end 2×100 bp sequence. 60 M total reads were acquired for each library. Three to five biological replicates were included in each group.

2.5 | RNA Sequencing Analysis

Bases with quality scores less than 30 and adapters were trimmed from raw sequencing reads by Trim Galore (v0.6.4). After trimming, reads with lengths greater than 30 bp were mapped to mm10 by STAR (v2.7.1a). Raw counts and normalized counts for each gene were produced by RSEM (v1.2.28). Batch effects were removed with the ComBat_seq function from the package sva (v3.46.0). Following batch effect removal, the distinction between the two batches was no longer discernible in the PCA plot (Figure S1). The raw counts were used to identify differentially expressed genes (DEGs) using DESeq2 (v1.36.0). Only genes with an adjusted p value less than 0.05 and at least a 1.5-fold change were considered DEGs. GO analysis was performed with clusterProfiler (v4.6.2) and org.Mm.eg.db (v3.16.0). ClueGO (v2.5.10) (Bindea et al. 2009) was used to summarize the GO terms. Mfuzz (v2.58.0) (Futschik and Carlisle 2005; Kumar 2007) was used to cluster genes based on the expression pattern.

3 | Results

Rodent astrocytes are born in the cortex postnatally and undergo migration, proliferation, and maturation during the first month of life (Akdemir et al. 2020; Clavreul et al. 2022; Sofroniew and Vinters 2010). Subsequently, each astrocyte continues to develop, mature, and age in its specific location until the end of its lifespan. Here, we evaluated the astrocyte transcriptome during early cortical development through young adulthood (P7, P14, P21, P28, and P60) and from adulthood through the aging process (3, 9, 12, and 18 months) in the male mice (Figure S1).

3.1 | Early Developmental Profiling of the Astrocyte Transcriptome in the Male Mouse Cortex

We first evaluated general postnatal developmental gene expression patterns in acutely isolated astrocytes from healthy, WT male mice. Astrocytes were collected longitudinally across early postnatal development and through young adulthood, enabling the evaluation of gene expression through the critical developmental period between birth and maturation (P7, P14, P21, P28, and P60). Over 20,000 protein-coding genes were detected at each time point (Table S1). The top 10 genes with the highest expression at each time point are shown (Figure 1A). Interestingly, four genes (*Apoe, Cst3, Mt1*, and *Ckb*) were consistently highly expressed during early development (Figure 1B). Notably, apolipoprotein E (*Apoe*), a lipid transporter, and cystatin C (*Cst3*), which serve an important physiological role as a local regulator of this enzyme activity, consistently showed the highest expression at each early time point examined, and the expression of each of these genes was relatively stable at each of these time points. These findings support previous findings on actively transcribed mRNAs in astrocytes (Farhy-Tselnicker et al. 2021). Additionally, the protein encoded by *Ckb* plays a central role in the regeneration of ATP in the brain (Kuiper et al. 2009), and the protein encoded by the *Mt1* gene acts as an antioxidant and protects against hydroxyl free radicals, which are important in the homeostatic control of metal in the cell (Swindell 2011; West et al. 2008).

To investigate differential gene expression during early development, we performed pairwise comparisons between adjacent time points with the criteria of adjusted p value <0.05 and log2 foldchange >1.5 (Table S2). The number of upregulated and downregulated DEGs for each comparison is presented in Figure 1C,D. Notably, we identified the highest number of differentially expressed genes (DEGs) between P14 and P21 (1164 DEGs) (Figure 1C,D), while a comparison of astrocytes between P21 and P28 demonstrated similar mRNA expression levels (Figure 1C). These results suggest the early maturation phase (P7–P21), when astrocytes undergo profound morphological changes (Bushong et al. 2004; Bushong et al. 2002; Farhy-Tselnicker and Allen 2018; Freeman 2010; Zarei-Kheirabadi et al. 2020), is associated with the most robust changes in gene expression, with the majority of genes being upregulated. By overlapping all the DEGs from the four comparisons, *Igfbp3* (insulin-like growth factor-binding protein 3) was found to be the only gene changing consistently during each early developmental period (Figure 1D). We conducted qPCR to further

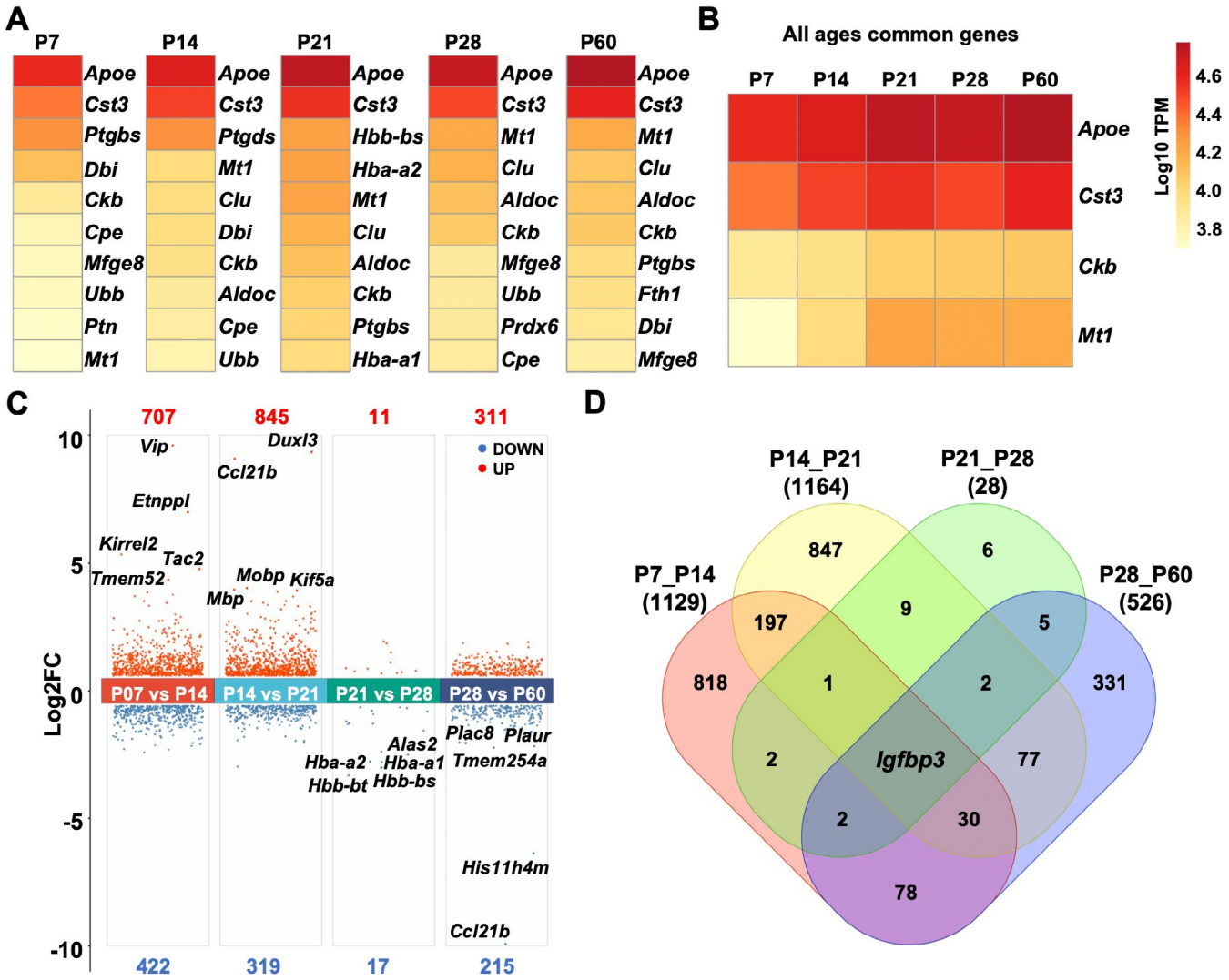

FIGURE 1 | Astrocyte transcriptome changes during early developmental. (A) Heatmaps of the top 10 genes expressed in astrocytes at each age, sorted by expression level. The colors represent the log10 TPM of the expression level. (B) Four genes commonly expressed at all ages. The colors represent the log10 TPM of the expression level. (C) Total upregulated and downregulated DEGs (p.adj value <0.05, log2 fold change >1.5). (D) Overlapping differentially expressed genes (DEGs) among all comparisons.

validate the expression of *Igfbp3* at various developmental time points. Consistent with the sequencing results, we observed a significant increase in *Igfbp3* levels from P7 to P21, followed by a decrease from P21 to P60. (Figure S2).

By plotting the gene expression change of all the DEGs during development (Figure S3), we observed distinct patterns of expression. To analyze these patterns in detail, we grouped the DEGs into four clusters based on their expression profiles (Figure 2A–H, Tables S3 and S4). Cluster 1, comprising 728 genes, displayed the highest expression at P7, followed by a consistent decrease from P7 to P21, and then maintained a relatively low but stable expression level until P60 (Figure 2A,B). Pathway enrichment analysis of Cluster 1 genes revealed associations with cell proliferation and developmental processes (Figure 2I). Notably, genes involved in the mitotic cell cycle process pathways demonstrated downregulation from P14, corroborating previous findings that astrocyte proliferation is largely complete by the end of the second postnatal week (Akdemir et al. 2020; Clavreul et al. 2022; Sofroniew and Vinters 2010; Vasile et al. 2017; Zhou et al. 2019). Clusters 2 and 3 showed similar expression change patterns (Figure 2C–F). Cluster 2 included 685 genes, while Cluster 3 comprised 690 genes. Both clusters exhibited a consistent increase in expression levels from P7 to P21, stabilizing at P28. However, Cluster 2 genes continued to increase from P28 to P60, whereas Cluster 3 genes decreased during this period. Pathway enrichment analysis indicated that genes in Clusters 2 and 3 are associated with synaptic signaling, dendrite development, cell communication, and cytoskeletal and cellular organization (Figure 2J,K). These findings align with previous studies highlighting P7 to P21, particularly P14 to P21, as critical periods for astrocyte morphological maturation and interaction with synaptic structures (Akdemir et al. 2020; Clavreul et al. 2022; Sofroniew and Vinters 2010; Vasile et al. 2017; Zhou et al. 2019). Cluster 4, the smallest cluster with 303 genes, exhibited low expression at P7, peaking at P14 and P28, and then declining to a minimum level at P60 (Figure 2G,H). Pathway analysis reveals that these genes are involved in biological processes like endothelial cell and blood vessel development (Figure 2L), which indicates that between P14 and P28, when astrocytes start to show

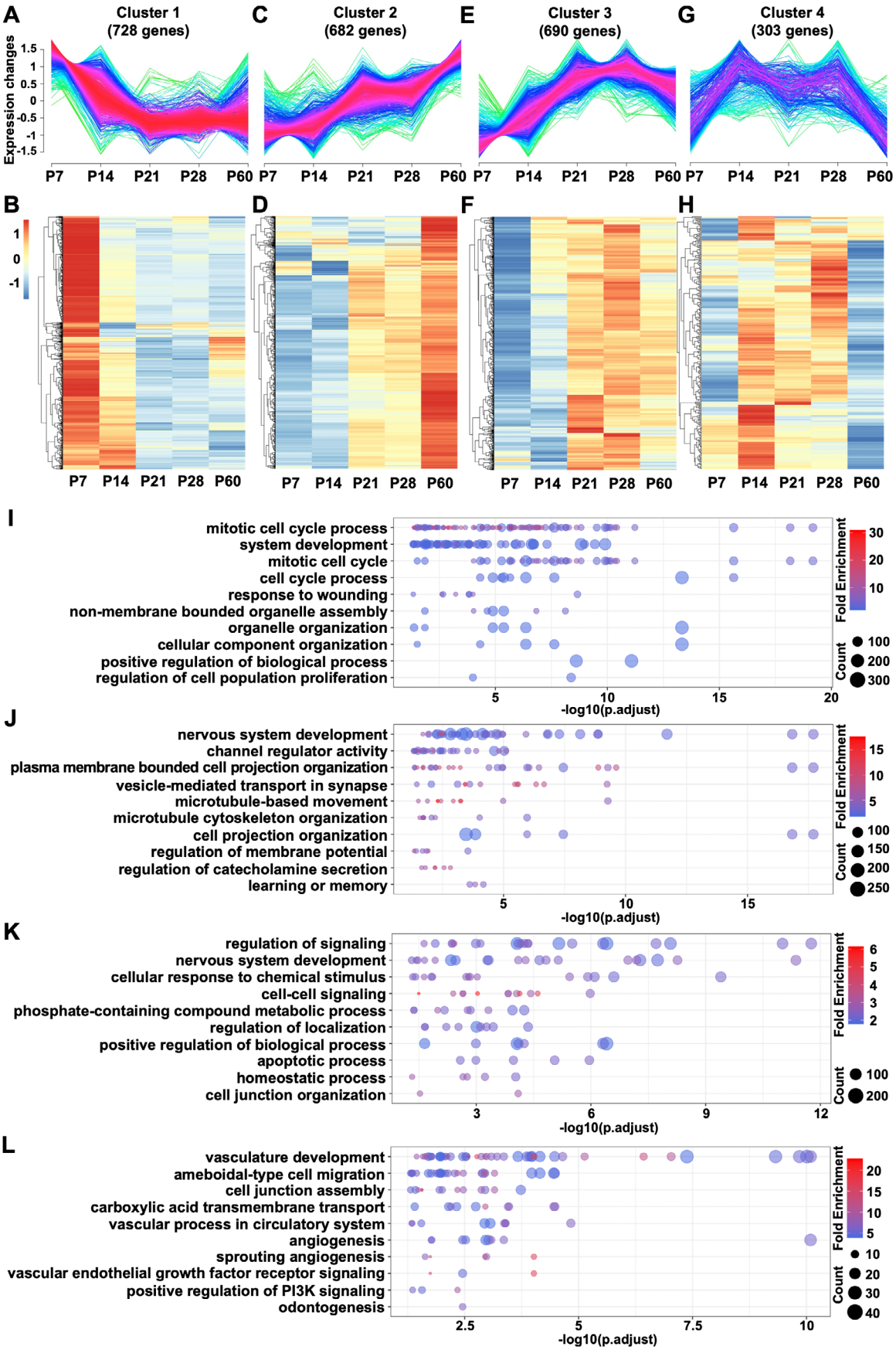

FIGURE 2 | Legend on next page.

FIGURE 2 | Astrocyte DEG expression trajectories during development. (A, C, E, G) Clusters of expression trajectories of DEGs throughout the astrocyte developmental process (P7, P14, P21, P28, and P60): Cluster 1 (A), Cluster 2 (C), Cluster 3 (E), and Cluster 4 (G). (B, D, F, H) Heatmaps of the expression of DEGs involved in each cluster: Cluster 1 (B), Cluster 2 (D), Cluster 3 (F), and Cluster 4 (H). The colors represent the log10 TPM of the expression level. (I–L) Top 10 most significant GO terms enriched with DEGs involved in Cluster 1 (I), Cluster 2 (J), Cluster 3 (K), and Cluster 4 (L). Each bubble represents a GO subterm. The colors represent the fold enrichment. The size of the bubble represents the number of genes.

mature morphology, their end-feet process begins to participate in blood–brain barrier (BBB) maintenance. The pattern of gene expression and pathway analysis in this cluster supports previous work which indicates that although astrocytes contribute to BBB development and maintenance from birth onward, astrocyte endfoot blood vessel coverage continues to mature through adulthood (Obermeier et al. 2013; Saili et al. 2017).

3.2 | Normal Aging Profiling of the Astrocyte Transcriptome in the Male Mouse Cortex

Matured astrocytes are essential in maintaining the health of the brain microenvironment. To investigate the transcriptome changes in astrocytes during normal aging, we selected four time points, 3, 6, 12, and 18 months, and performed RNA-seq for cortical astrocytes (Table S1). Similar to the top 10 genes with the highest expression in the developmental transcriptomes, *Apoe*, *Cst3, Ckb, and Mt1* were prominently expressed in aging astrocyte transcriptomes (Figure 3A,B). Notably, *Apoe* and *Cst3* were the top two genes expressed across all developmental and aging groups, underscoring their critical roles in sustaining fundamental astrocyte functions. Additionally, *Clu* (Clusterin) and *Aldoc* (Aldolase, Fructose-Bisphosphate C) were identified as common genes during aging (Figure 3B), and both are listed among the top 10 genes with the highest expression from P14 onward. In the brain, *Clu* is a secreted glycoprotein that has been shown to enhance neuronal differentiation (Cordero-Llana et al. 2011) is also a associated with lipid transport (Baralla et al. 2015; Matukumalli et al. 2017), while genetic variation of this gene is associated with Alzheimer's disease (Chen et al. 2021; Guerreiro et al. 2010). *Aldoc* has been used as a marker to identify astrocytes (Tsai et al. 2012) and participates in the glycolysis pathway in the brain (Xiong et al. 2022).

By comparing the developmental and aging transcriptomes of astrocytes, we observed that Apoe, Cst3, Ckb, and Mt1 maintain high expression levels during both early developmental stages and aging. To explore the roles of genes consistently highly expressed in mature astrocytes, we selected four time points representing healthy adult mature astrocytes (P28, P60, 3 months, and 6 months) and identified 417 overlapping genes from the top 500 genes at each time point. Pathway analysis revealed that these genes primarily support basic cellular functions. Moreover, processes related to cellular respiration, especially the aerobic respiration process ("aerobic respiration", "glucose catabolic process," "regulation to oxygen-containing compound," and "tricarboxylic acid cycle"), were enriched with these genes (Figure 3C), reinforcing the role of astrocytes in brain energy metabolism (Belanger et al. 2011). Additionally, adult astrocytes were found to regulate plasma lipoprotein levels (Figure 3C), supporting their function in lipid and cholesterol metabolism and transport (Pfrieger and Ungerer 2011).

DEGs were identified between adjacent time points (Table S2). Unlike the majority of genes upregulated during development, 430 out of 77 DEGs were downregulated in astrocytes at 6 months compared with those at 3 months (Figure 3D). The gene expression levels in 6 and 12 months astrocytes were very similar, with only 18 DEGs identified between these two time points. In contrast, a greater number of DEGs were identified between 12 and 18 months, with 304 DEGs upregulated and 342 DEGs downregulated. Notably, *Etv4* (ETS translocation variant 4, also known as PEA3) and *Crim1* (cysteine-rich motor neuron 1 protein) were consistently altered during astrocyte aging (Figure 3E). *Etv4* is a critical component of a gene network downstream of the BDNF/TrkB pathway (Fontanet et al. 2018). *Crim1* directs thoracolumbar axon extension in corticospinal neurons (Sahni et al. 2021), although its function in astrocytes remains unclear. Validation using qPCR demonstrates a significant increase in *Crim1* levels from 3 to 6 months, followed by a decrease from 6 to 12 months, and a subsequent increase from 12 to 18 months (Figure S2).

Similarly, the DEGs associated with astrocyte aging exhibited distinct expression patterns (Figure S3). These DEGs were categorized into four clusters based on their expression patterns (Figure 4A–L, Tables S5 and S6). Cluster 1 comprised 291 genes with relatively stable expression levels from 3 to 12 months, followed by a substantial increase at 18 months (Figure 4A,B). These genes are associated with peptidase activity and regulation of apoptosis, potentially contributing to the aging process (Figure 4I). Conversely, the 195 genes in Cluster 2 showed a decreasing trend from 3 to 18 months (Figure 4C,D), and are involved in pathways related to the mitotic cell cycle process (Figure 4J). Cluster 3, containing 305 genes, exhibited the lowest expression level at 6 months with a slight increase from 6 to 18 months (Figure 4E,F). Pathway analysis suggested that Cluster 3 genes may be linked to axonemal assembly and microtubules, indicating potential morphological changes in aging astrocytes (Figure 4K). The 342 genes in Cluster 4 showed the highest expression at 12 months, followed by a decrease to the lowest level at 18 months (Figure 4G,H). Pathways enriched in Cluster 4 indicate that gene expression changes could be associated with reduced lipid synthesis, transport, and cell activity in aging astrocytes (Allende et al. 2024; Ferris et al. 2017; Lee et al. 2021) (Figure 4L).

3.3 | Expression Change of Astrocyte Functional Genes During Early Development and Aging

By analyzing transcriptome data from astrocytes at different developmental stages, we assessed the changes in the expression of genes crucial for astrocyte function across the lifespan. The genes evaluated included astrocyte markers (*Aldh1l1, Ezr, S100b, Aldoc, Ndrg2, Sox9, Lhx2, Gfap, Vim*), astrocyte aquaporins (*Aqp9, Aqp4*), subunits of astrocyte GABA receptors

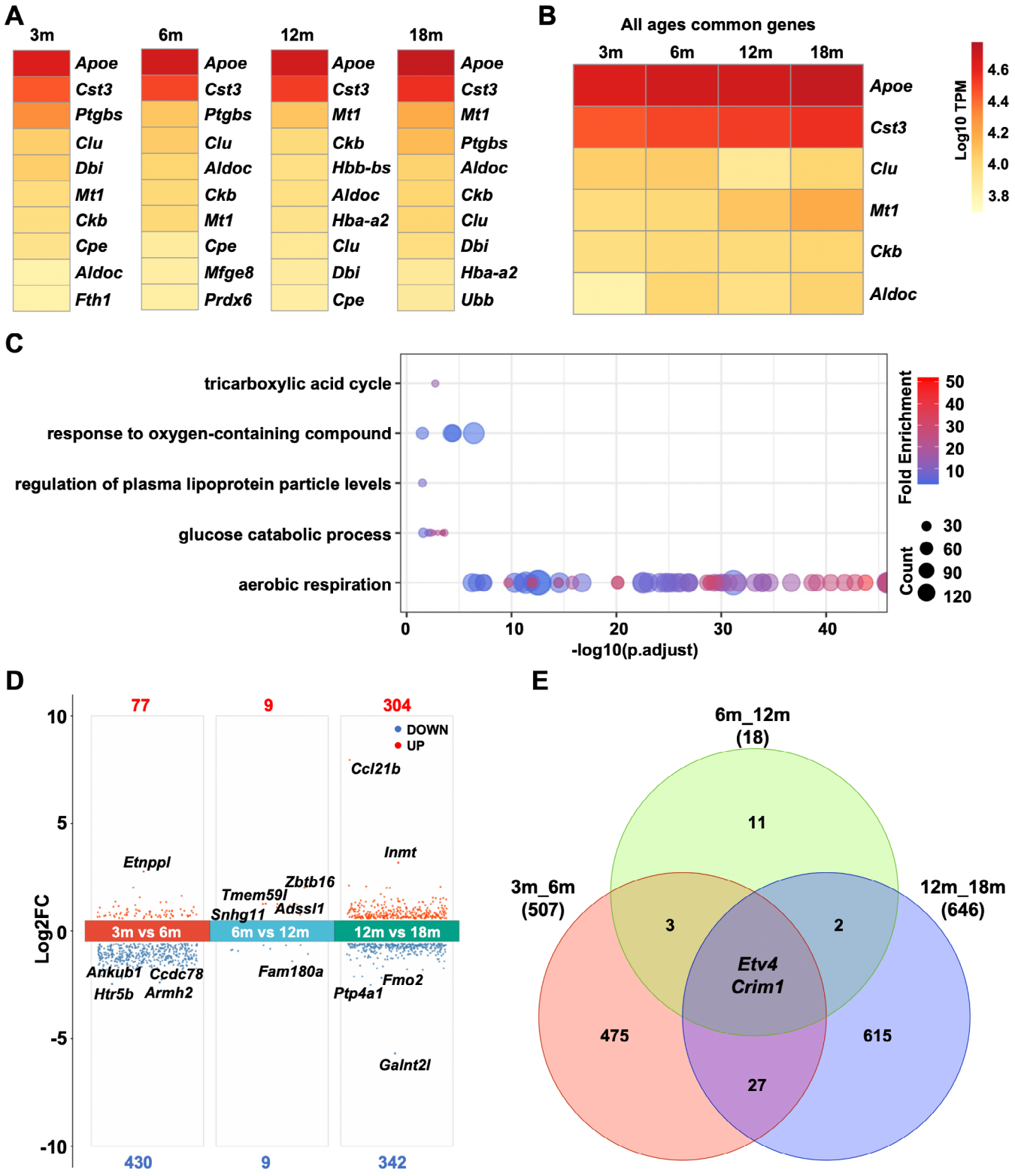

FIGURE 3 | Astrocyte transcriptome changes during aging. (A) Heatmaps of the top 10 genes expressed in astrocytes at each age, sorted by expression level. The colors represent the log10 TPM of the expression level. (B) Six genes commonly expressed at all ages. The colors represent the log10 TPM of the expression level. (C) Pathway analysis of the overlapping highly expressed genes (top 500 genes) in the adult period (P28, P60, 3 months, and 6 months). Each bubble represents a GO subterm. The colors represent the fold enrichment. The size of the bubble represents the number of genes. (D) Total upregulated and downregulated DEGs (p.adj value <0.05, log2-fold change >1.5). (E) Overlapping differentially expressed genes (DEGs) among all comparisons.

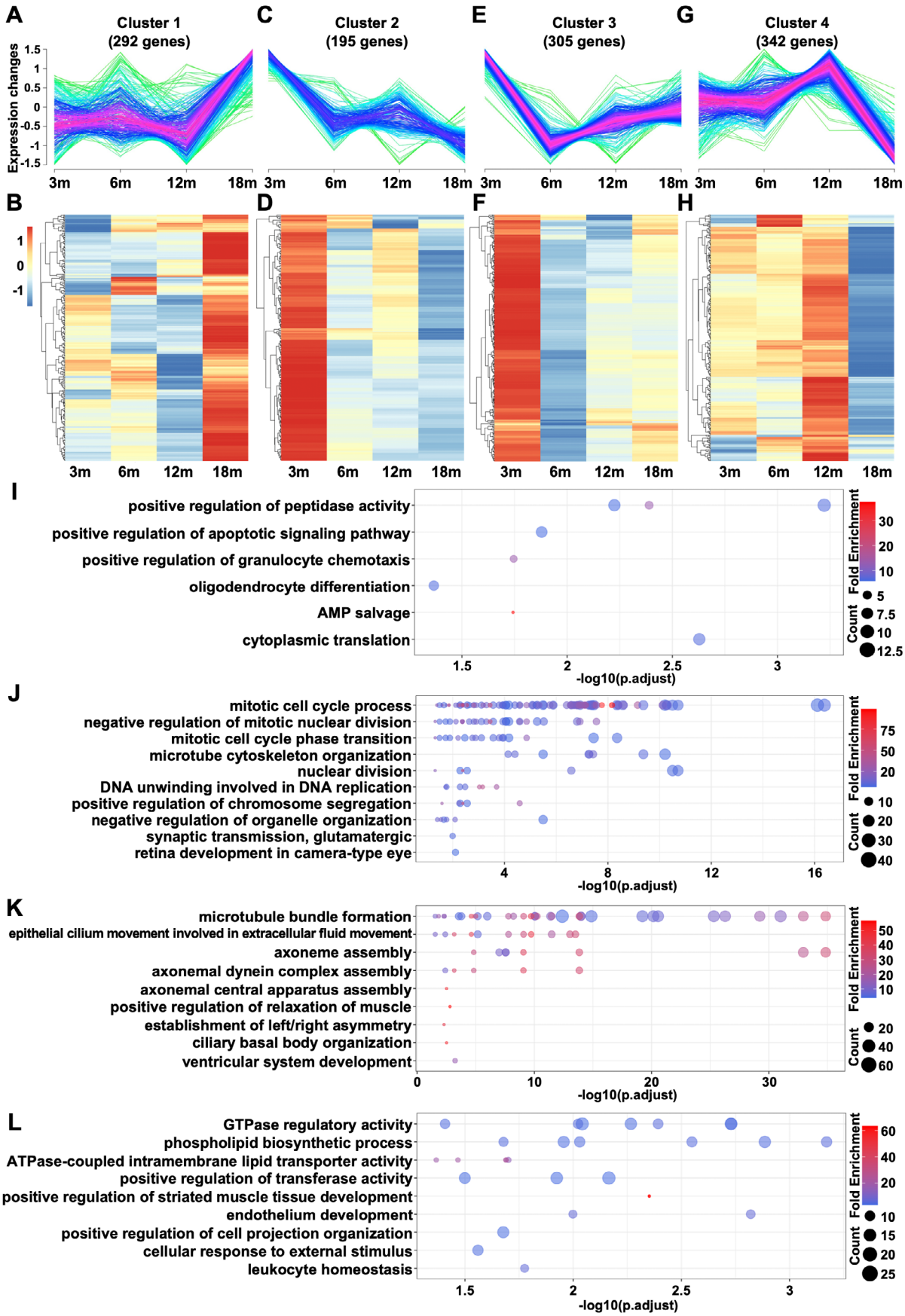

FIGURE 4 | Legend on next page.

FIGURE 4 | Astrocyte DEG expression trajectories during aging. (A, C, E, G) Clusters of expression trajectories of DEGs throughout the astrocyte aging process (3, 6, 12, and 18 months): Cluster 1 (A), Cluster 2 (C), Cluster 3 (E), and Cluster 4 (G). (B, D, F, H) Heatmaps of the expression of DEGs involved in each cluster: Cluster 1 (B), Cluster 2 (D), Cluster 3 (F), and Cluster 4 (H). The colors represent the Log10 TPM of the expression level. (I–L) Top 10 most significant GO terms enriched with DEGs involved in Cluster 1 (I), Cluster 2 (J), Cluster 3 (K), and Cluster 4 (L). Each bubble represents a GO subterm. The colors represent the fold enrichment. The size of the bubble represents the number of genes.

(*Gabra2, Gabra4, Gabrb1, Gabrg1, Babbr1, Gabbr2*), astrocyte GABA transporters (*Slc6a1, Slc6a11*), astrocyte potassium (K^+) channels (*Kcnk1, Kcnk2, Kcnk10, Kcnj10, Kcnj16*), astrocyte glutamate uptake (*Slc1a3, Slc1a2, Grm3, Grm5, Gria2, Glul*), and astrocyte glutamate release (*Vamp2, Vamp3, Stx1a, Snap25, Snap23, P2rx7*). These genes were selected based on previous studies (Liu et al. 2022; Mahmoud et al. 2019; Olsen and Sieghart 2008; Rusnakova et al. 2013). To investigate the expression changes of these genes across the lifespan of astrocytes, we used P7 as the baseline and calculated the log2-fold change at all other time points relative to P7. Comparative analysis of gene expression across different age groups was conducted with respect to the P7 baseline, and the results were visualized using heatmaps (Figure 5A–F). Four genes were selected for validation using qPCR: *Gfap, Aqp4, Kcnk1*, and *Snap25*. All of these genes exhibited consistent changes in expression patterns that aligned with the sequencing results (Figure S2).

Our findings indicate that these marker genes exhibit distinct expression patterns from early to late time points (Figure 5A). Among the astrocyte markers, *Aldh1l1* (aldehyde dehydrogenase 1 family member L1) showed the most stable expression, highlighting its value as a marker for astrocyte identification across all developmental and aging stages. *S100b* (S100 calcium-binding protein B) and *Ezr* (Ezrin) (Lavialle et al. 2011), which are localized to astrocyte fine processes and endfeet, consistently presented relatively high expression levels at time points other than P7. *Aldoc* (aldolase, fructose-bisphosphate C), which presented the highest expression level among the markers at P7, and *Ndrg2* (N-Myc downstream-regulated gene 2) (Flügge et al. 2014) were more recently described as astrocyte markers localized to the nucleoplasm. These two genes were upregulated during early development, with expression levels remaining similar to P7 during aging, suggesting that these genes are related to astrocyte differentiation and maturation. The transcription factors *Sox9* (SRY-Related HMG Box Gene 9) and *Lhx2* (LIM Homeobox 2) (Shaltouki et al. 2013), located in the nucleus, maintained stable expression from P7 to P14, with increased levels at later time points compared to P7. The cytoskeleton-related astrocyte markers *Gfap* (glial fibrillary acidic protein) and *Vim* (Vimentin) peaked at P7, with expression levels decreasing at later time points. This data may guide the future selection of astrocyte markers based on developmental stages.

Astrocytes are highly specialized glial cells that sense and respond to a variety of signals, primarily through receptors, channels, and transporters. Aquaporins represent a family of channels associated with the movement of water molecules across the lipid bilayer. In astrocytes, aquaporins localize to the astrocyte endfeet that enwrap the vasculature. Specifically, Aquaporin-4 (*Aqp4*) and Aquaporin-9 (*Aqp9*) are expressed in astrocytes, with *Aqp4* exhibiting higher expression levels than *Aqp9* at P7. The expression of *Aqp9* remains relatively stable, except for a decrease observed at 18 months, whereas *Aqp4* expression starts to decrease from P60 onward, whereby in both immature and mature astrocytes, the expression of *Aqp4* is at least 40× the level of *Aqp9*. (Figure 5B). We also investigated the expression changes of two important K^+ channels, the two-pore domain K^+ channels and inwardly rectifying K^+ channels, by profiling the expression of five related genes. Among the genes encoding two-pore domain K^+ channels, *Kcnk1* showed the highest expression level at P7 compared to *Kcnk2* and *Kcnk10*, with a significant increase reaching its peak at P28. For the inwardly rectifying K^+ channel, *Kcnj16* displayed higher expression levels compared to *Kcnj10*, with increased levels observed from P21 onward (Figure 5C). In addition, *Kcnj10* and *Kcnj16* are both highly expressed in immature astrocytes, whereas *Kcnj16* is dominant in mature astrocytes. Given that heteromeric Kir4.1/5.1 and homomeric Kir4.1 have different ion channel properties (Hibino et al. 2005; Pessia et al. 2001), this differential expression of K^+ channels may influence the uptake and distribution of high extracellular K^+ by astrocytes during development and aging.

γ-Aminobutyric acid (GABA) is the major inhibitory neurotransmitter in the brain. Astrocytes express both GABA transporters and receptors to help maintain GABA homeostasis. We found that the GABA transporters, such as GAT-1 (*Slc6a1*) and GAT-3 (*Slc6a11*), were highly expressed at P7, with increased expression levels in subsequent stages. Among the GABA receptor subunits, GABAA receptor α subunits 2 and 4 (*Gabra2* and *Gabra4*), β subunit 1 (*Gabrb1*), γ subunit 1 (*Gabrg1*), and both GABAB receptor subunits B1 (*Gabbr1*) and B2 (*Gabbr2*) were highly expressed in astrocytes (Figure 5D). Notably, *Gabra4* and *Gabbr1* showed relatively stable expression, while *Gabrg1* and *Gabrb1* exhibited higher expression levels at later time points compared to P7. *Gabra2* was upregulated during the development stage, and *Gabbr2* expression remained stable in developmental astrocytes but was upregulated in adult astrocytes.

Glutamate is the most abundant excitatory neurotransmitter in the brain, and astrocytes are primary regulators of neuronally released glutamate. Two important astrocytic glutamate transporters are GLAST (*Slc1a3*) and GLT-1 (*Slc1a2*). *Slc1a3* is abundantly expressed at P7 and maintains a stable expression level throughout the lifespan of astrocytes, while *Slc1a2* expression is consistently higher than that at P7, increasing with age (Figure 5E). Metabotropic glutamate receptor 3 (mGluR3) and metabotropic glutamate receptor 5 (mGluR5), encoded by genes *Grm3* and *Grm5*, are two important G protein-coupled receptors expressed in astrocytes. Our analysis indicates that *Grm3* expression is higher than *Grm5* and exceeds P7 levels at most observed time points, whereas *Grm5* expression is lower in the later stages compared to P7 (Figure 5E). For glutamate-gated ion channels, AMPA (α-amino-3-hydroxy-5-methyl-4-isoxazolepropionic

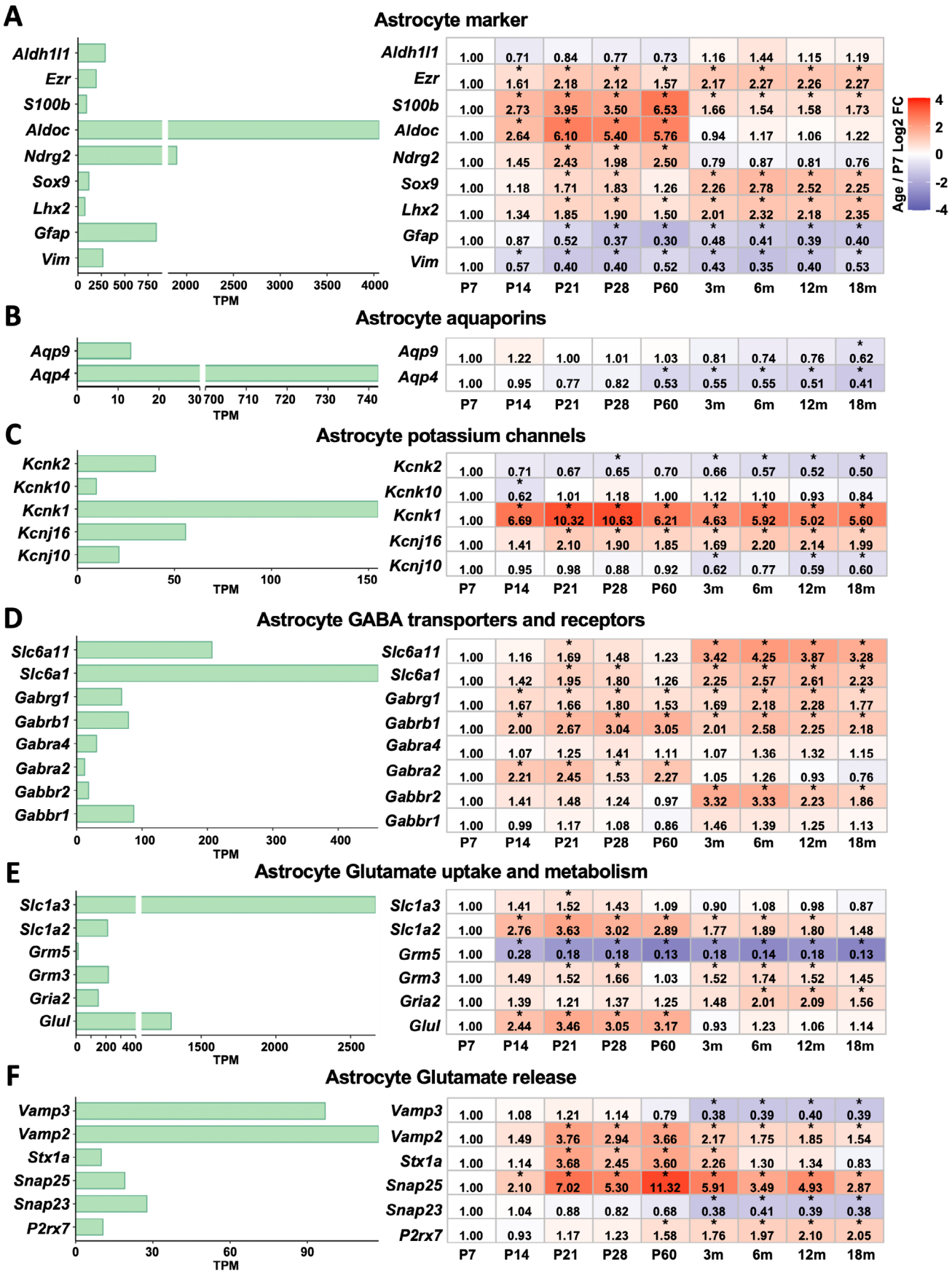

FIGURE 5 | Legend on next page.

FIGURE 5 | Astrocytic function and structural gene changes. (A–F) Bar plots (left) and heatmaps (right) of selected genes related to astrocyte markers (A), aquaporins (B), potassium channels (C), GABA transporters and receptors (D), glutamate uptake and metabolism (E), and glutamate release (F) expression plotted as TPM at P7 (left) and plotted as log2-fold change (FC) at each age relative to P7 (right). The colors represent upregulated (red) and downregulated (blue) genes. Genes with *p*.adj value < 0.05 and log2FC > 1.5 compared with P7 at each age were marked with star. The numbers represent the FC of each gene at different time points compared with P7.

acid) receptors, astrocytes predominantly express subunit 2 GluA2 (*Gria2*). *Gria2* expression remains similar from P7 to 3 months and increases starting from 6 months compared to P7 (Figure 5E), consistent with previous findings by Molders et al. (2018). This suggests that AMPA receptors in WT astrocytes are impermeable to Ca^{2+}. Astrocytes play a critical role in maintaining glutamatergic transmission homeostasis by replenishing glutamate through the glutamate/glutamine cycle. Glutamine synthetase (GS), encoded by *Glul* and produced by astrocytes, is essential for this cycle. *Glul* expression is higher than P7 during early development and maintains a similar level during aging (Figure 5E).

Although controversial, astrocytes are implicated in the regulation of neuronal activity through the release of glutamate, primarily via calcium (Ca^{2+})-mediated exocytosis under physiological conditions (Mahmoud et al. 2019). The expression levels of vesicle-associated membrane protein 2 (*Vamp2*) and vesicle-associated membrane protein 3 (*Vamp3*) are notably higher compared to other related genes (Figure 5F). Both *Vamp2* and synaptosomal-associated protein 25 (*Snap25*) are upregulated at various time points compared to P7. Syntaxin-1 (*Stx1a*) level is elevated from P21 to 3 months. Synaptosomal-associated protein 23 (*Snap23*) maintains a stable expression level until P60, after which it decreases starting from 3 months. Another receptor involved in the glutamate release pathway, P2X purinoceptor 7 encoded by *P2rx7*, which facilitates glutamate release by triggering Ca^{2+}-dependent exocytosis and serving as a pathway for non-exocytotic glutamate release from neurons or astrocytes, shows a contrasting expression pattern to *Snap23*. *P2rx7* expression remains consistent during developmental stages and increases after P60, highlighting its crucial role in mature astrocytes (Figure 5F). These data demonstrate that at the gene level, astrocytes may contain the cellular machinery for vesicular glutamate release.

3.4 | Shorter Transcripts Are Preferred in Aged Astrocytes

Previous studies have identified a systematic phenomenon known as gene-length-dependent transcription decline (GLTD), which is characterized by a reduction in the expression of long genes in the aging brain, as observed in both normal aging and neurodegenerative diseases (Soheili-Nezhad et al. 2024; Soheili-Nezhad et al. 2021). Our gene ontology (GO) analysis of aged animals similarly revealed the enrichment of pathways associated with DNA damage and DNA-binding transcription factor activity (Table S7). These findings prompted us to further investigate transcript length changes in aged astrocytes, which have not been previously explored. We compared the distribution of transcript lengths expressed (TPM > 10) across all time points. The distribution of transcript lengths was similar across most time points, with the exception of the 18 months time point. Compared to the transcript length distribution at 18 months, younger time points, P7 and P14, did not demonstrate significant differences (Figure 6A). However, significant differences were observed in transcript length distribution in adolescent and adult astrocytes (from P21 to 12 months) relative to 18 months (Kolmogorov–Smirnoff tests, $p < 0.05$). Astrocytes at 18 months tended to express more short transcripts and fewer long transcripts.

To further evaluate the genes contributing to differences in transcript length, we compared gene expression in astrocytes at 3 and 6 months with those at 18 months. These time points represent relative stability in gene expression during early adulthood compared to that of aged animals. We first examined shorter transcripts (transcript length 400–2000 bp, based on the intersection points of the curves) expressed in 18 months but absent in 3 and 6 months astrocytes. We identified 39 and 80 such transcripts when comparing 18 to 3 months and 6 months astrocytes, respectively. GO analysis of transcripts unique to 18 months compared to 3 months revealed functions related to immune system regulation, response to DNA damage, and biotic stimulus response regulation (Figure 6B). This reflects the complex interplay of aging processes affecting various physiological pathways. Shorter transcripts unique to 18 months when compared to 6 months astrocytes were associated with DNA biosynthesis processes and assembly of organelle and axoneme (Figure 6C). This indicates potential repair mechanisms for damage and morphological changes in aged astrocytes.

We then analyzed longer transcripts (transcript length 2700–11,750 bp) present in 3 and 6 months astrocytes but missing in 18 months astrocytes. These genes were mainly related to synaptic structure and function and neurotransmitter regulation. This indicates that as astrocytes age, they may alter synaptic support (Figure 6D,E).

4 | Discussion

In this study, we profiled the astrocyte transcriptome from the male mouse cortex across the lifespan, ranging from postnatal day (P) 7 to 18 months. Our data revealed that the majority of the gene expression changes occurred between P7 and P21 during the developmental stage, with most genes showing an increasing trend. During the aging process, astrocytes at 6 and 12 months exhibit similar mRNA levels, whereas the genes altered between 12 and 18 months are predominantly downregulated. Gene expression levels in the adult stage (P60 to 3 months) remain relatively stable compared to other developmental periods. Notably, 417 genes were consistently ranked among the top 500 expressed genes at these time points, playing essential roles in supporting the fundamental cellular functions of astrocytes.

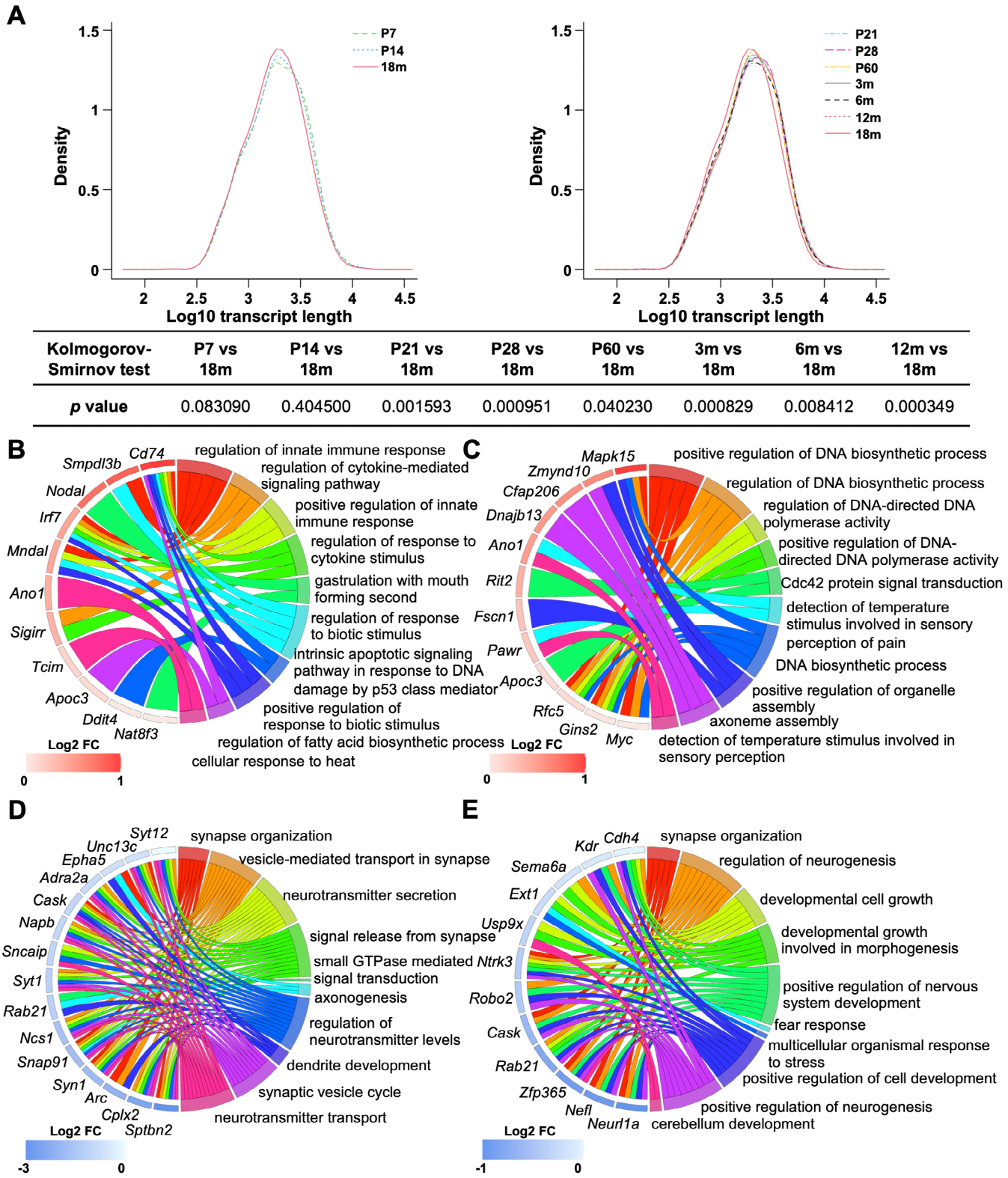

Kolmogorov-Smirnov test	P7 vs 18m	P14 vs 18m	P21 vs 18m	P28 vs 18m	P60 vs 18m	3m vs 18m	6m vs 18m	12m vs 18m
p value	0.083090	0.404500	0.001593	0.000951	0.040230	0.000829	0.008412	0.000349

FIGURE 6 | Shorter transcripts tend to be more highly expressed in 18 months astrocytes. (A) Astrocyte transcript distributions of different comparisons. The Kolmogorov–Smirnov test was performed to evaluate the difference in transcript length distribution at different time points. (B–C) Top 10 most significant GO terms enriched with short transcripts comparing 3 and 18 months (B), 6 and 18 months (C), and related genes. Foldchange represents the change in 18 months compared with 3 or 6 months. (D–E) Top 10 most significant GO terms enriched with long transcripts comparing 3 and 18 months (D), 6 and 18 months (E), and related genes. The fold change represents the change at 18 months compared with 3 or 6 months.

During development, we observed that the majority of gene expression changes occurred earlier, between P7 and P21. Only 28 genes showed significant changes between P21 and P28. This limited transcriptional shift may reflect a period of relative stability as astrocytes transition from active developmental processes, such as proliferation and differentiation, to the consolidation of

their functional and structural roles. Previous studies suggest that astrocytes show mature morphology characteristics by the third postnatal week (Bushong et al. 2004; Bushong et al. 2002; Farhy-Tselnicker and Allen 2018; Zarei-Kheirabadi et al. 2020), which could account for the reduced transcriptional dynamics during this period. Additionally, the 7-day interval between P21 and P28 at this developmental stage may be insufficient to capture substantial gene expression changes, potentially explaining the more pronounced shifts observed between P28 and P60 (32-day interval). While in the aging process, more genes changed between 3 and 6 months compared to 6 and 12 months. This may be related to the continued functional maturation and optimization of astrocytes in early adulthood. This period may involve the fine-tuning of astrocyte roles in synaptic support, metabolic regulation, and neurovascular coupling. By 6 months, astrocytes appear to enter a more stable phase to maintain the mature CNS. The changes between 12 and 18 months may indicate the onset of aging-related processes. The validity of the sequencing data was confirmed through qPCR. However, complementary techniques such as RNAscope or immunohistochemistry, which provide spatial context, could offer further insights into the cellular localization of these gene products within the tissue.

A particularly interesting gene observed during the developmental stage is *Igfbp3*, which showed consistent change from P7 to P60. *Igfbp3* is a member of the insulin-like growth factor binding protein (IGFBP) family and contains both an IGFBP and a thyroglobulin type-I domain. The IGFBP family plays a crucial role in brain development and function. For instance, astrocyte-secreted IGFBP2 has been shown to mediate neuronal development (Caldwell et al. 2022). *Igfbp3* has been confirmed to be directly regulated by *Mecp2*, a causative gene of Rett syndrome (Itoh et al. 2007). Moreover, insulin-like growth factor 1 (IGF1), which predominantly binds to IGFBP3 (Endogenous et al. 2010), has been employed in the treatment of Rett syndrome model mice, resulting in partial improvement of behavioral and neurologic symptoms in these animals (Castro et al. 2014). These findings underscore the important role of astrocytes in early brain development and suggest potential therapeutic targets in astrocytes for neurological diseases.

Our results confirmed the expression of several newly identified astrocyte markers, including *Ezr, Aldoc, Ndrg2*, and *Lhx2*. Previous studies have indicated that *Aldoc* is predominantly expressed in subpopulations of cerebellar Purkinje cells (PCs) (Fujita et al. 2014). Our transcriptomic data revealed that *Aldoc* exhibited higher expression levels compared to other commonly used astrocyte markers at P7 in WT cortical astrocytes and ranked among the top 10 expressed genes in astrocytes across most time points. This finding suggests that *Aldoc* is also highly expressed in cortical astrocytes and could serve as a reliable astrocyte marker in future studies. We clustered these astrocyte markers into different groups based on their subcellular locations. Interestingly, their expression patterns varied during development and aging. *Aldh1l1* expression remains stable throughout early development and aging, making it a robust marker for both young and mature astrocytes. To identify astrocytes during early development, *Aldoc* and *Ndrg2* are preferable markers as their expression is upregulated from P7 to P60, returning to P7 levels after 3 months. Additionally, our data indicated that *Gfap* and *Vim* mRNA levels were highest during the first week after birth and declined as the animal matured, consistent with previous findings (Luo et al. 2017; Sarthy et al. 1991).

By analyzing gene expression profiles throughout the lifespan of astrocytes, we identified distinct gene clusters based on expression levels. During development, one significant cluster exhibited peak gene expression at postnatal days 14 (P14) and 28 (P28). Pathway analysis revealed that these genes are associated with endothelial cell and blood vessel development. This finding further supports the role of astrocytes in maintaining the blood–brain barrier (BBB) after birth, as the coverage of astrocytic endfeet on the BBB increases from 64% in newborn mice to 98% in adults (Obermeier et al. 2013; Saili et al. 2017). Additionally, our results suggest that BBB maturation in mice may occur around P28. Collectively, our analysis of the postnatal maturation period aligns with previous studies, reinforcing the timeline of astrocyte morphological maturation, BBB maintenance, and their critical functions. Another important observation from this analysis is that both Cluster 1 in development and Cluster 2 from aging are enriched for pathways related to cell proliferation. Notably, 75 genes overlap between these clusters, and pathway enrichment analysis highlights that the majority of the top pathways are involved in cell proliferation processes. Analysis of the genes within the 20 most significant pathways (all related to cell proliferation) revealed a progressive decline in expression as age increases (Figure S4), indicating reduced astrocyte proliferation activity with advancing age.

In our analysis of transcript length across different time points, we found that aged astrocytes tend to express shorter transcripts (400–2000 bp). This phenomenon may be universal across all aged cells, which may be the compensatory response to the increased cellular stress and damage associated with aging. Given the potential for DNA damage in aged cells, the expression of shorter transcripts could increase translation efficiency and rapid protein production, which could be crucial in maintaining cellular homeostasis under stress. The GO analysis further supports this, as the short transcripts uniquely expressed in 18 months astrocytes are predominantly involved in processes related to immune system regulation, the DNA damage response, and the response to biotic stimuli. These functions are critical in aging cells, where the accumulation of DNA damage and increased inflammatory responses are common. The fact that these shorter transcripts are upregulated in older astrocytes suggests that these cells may be actively engaged in protective and repair mechanisms to counteract the detrimental effects of aging.

In conclusion, the investigation of transcriptome changes in astrocyte development and aging has unveiled the intricate molecular dynamics underlying these processes. Although our astrocyte isolation and sequencing do not allow for tracking gene expression changes in specific astrocyte subtypes, our magnetic isolation approach enables us to capture both the soma and dense network of processes of astrocytes (Holt and Olsen 2016), enabling the analysis of mRNAs located in peripheral processes (Mazare et al. 2020; Sakers et al. 2017). This is critical given the fact that astrocyte processes comprise the majority of the cell volume. These data offer valuable insights into the overall transcriptional landscape throughout the astrocyte

lifespan, which enables the detection of subtle gene expression alterations in astrocyte developmental and aging processes and facilitates the identification of rare transcripts that may otherwise be missed. Our dataset not only validated decades of research on gene expression changes associated with astrocyte maturation and function but also enabled a detailed temporal profiling of astrocyte transcriptomes spanning from early development through aging. The identified gene expression patterns provide a foundation for further exploration into the functional significance of astrocytes in neural development, synaptic maintenance, and age-related neurological disorders. This study opens new avenues and new insights for targeted therapeutic strategies aimed at preserving astrocyte function and mitigating age-related neurodegeneration.

Author Contributions

X.W.: experimental design, data collection and analysis, figure generation, manuscript content creation and editing; J.L.: experimental design, data collection and analysis, figure generation, manuscript content creation and editing; M.L.O.: securing funding, experimental design, staff management, manuscript content creation and editing.

Acknowledgments

We thank Dr. Beatriz Pinkston for participating in the discussions related to manuscript preparation.

Ethics Statement

All mouse experimental protocols were followed according to NIH guidelines and received approval from the Animal Care and Use Committee of Virginia Tech.

Conflicts of Interest

The authors declare no conflicts of interest.

Data Availability Statement

The data that support the findings of this study are openly available in GEO database at https://www.ncbi.nlm.nih.gov/geo/query/acc.cgi?acc=GSE272573, reference number GSE272573.

References

Agulhon, C., J. Petravicz, A. B. McMullen, et al. 2008. "What Is the Role of Astrocyte Calcium in Neurophysiology?" *Neuron* 59, no. 6: 932–946. https://doi.org/10.1016/j.neuron.2008.09.004.

Akdemir, E. S., A. Y. Huang, and B. Deneen. 2020. "Astrocytogenesis: Where, When, and How." *F1000Research* 9: 233. https://doi.org/10.12688/f1000research.22405.1.

Allende, L. G., L. Natalí, A. B. Cragnolini, et al. 2024. "Lysosomal Cholesterol Accumulation in Aged Astrocytes Impairs Cholesterol Delivery to Neurons and Can Be Rescued by Cannabinoids." *Glia* 72, no. 10: 1746–1765. https://doi.org/10.1002/glia.24580.

Baralla, A., E. Sotgiu, M. Deiana, et al. 2015. "Plasma Clusterin and Lipid Profile: A Link With Aging and Cardiovascular Diseases in a Population With a Consistent Number of Centenarians." *PLoS One* 10, no. 6: e0128029. https://doi.org/10.1371/journal.pone.0128029.

Belanger, M., I. Allaman, and P. J. Magistretti. 2011. "Brain Energy Metabolism: Focus on Astrocyte-Neuron Metabolic Cooperation." *Cell Metabolism* 14, no. 6: 724–738. https://doi.org/10.1016/j.cmet.2011.08.016.

Bindea, G., B. Mlecnik, H. Hackl, et al. 2009. "ClueGO: A Cytoscape Plug-In to Decipher Functionally Grouped Gene Ontology and Pathway Annotation Networks." *Bioinformatics* 25, no. 8: 1091–1093. https://doi.org/10.1093/bioinformatics/btp101.

Boisvert, M. M., G. A. Erikson, M. N. Shokhirev, and N. J. Allen. 2018. "The Aging Astrocyte Transcriptome From Multiple Regions of the Mouse Brain." *Cell Reports* 22, no. 1: 269–285. https://doi.org/10.1016/j.celrep.2017.12.039.

Brandebura, A. N., A. Paumier, T. S. Onur, and N. J. Allen. 2023. "Astrocyte Contribution to Dysfunction, Risk and Progression in Neurodegenerative Disorders." *Nature Reviews Neuroscience* 24, no. 1: 23–39. https://doi.org/10.1038/s41583-022-00641-1.

Bushong, E. A., M. E. Martone, and M. H. Ellisman. 2004. "Maturation of Astrocyte Morphology and the Establishment of Astrocyte Domains During Postnatal Hippocampal Development." *International Journal of Developmental Neuroscience* 22, no. 2: 73–86. https://doi.org/10.1016/j.ijdevneu.2003.12.008.

Bushong, E. A., M. E. Martone, Y. Z. Jones, and M. H. Ellisman. 2002. "Protoplasmic Astrocytes in CA1 Stratum Radiatum Occupy Separate Anatomical Domains." *Journal of Neuroscience* 22, no. 1: 183–192. https://www.ncbi.nlm.nih.gov/pubmed/11756501.

Caldwell, A. L. M., L. Sancho, J. Deng, et al. 2022. "Aberrant Astrocyte Protein Secretion Contributes to Altered Neuronal Development in Multiple Models of Neurodevelopmental Disorders." *Nature Neuroscience* 25, no. 9: 1163–1178. https://doi.org/10.1038/s41593-022-01150-1.

Castro, J., R. I. Garcia, S. Kwok, et al. 2014. "Functional Recovery With Recombinant Human IGF1 Treatment in a Mouse Model of Rett Syndrome." *Proceedings of the National Academy of Sciences of the United States of America* 111, no. 27: 9941–9946. https://doi.org/10.1073/pnas.1311685111.

Chen, F., D. B. Swartzlander, A. Ghosh, J. D. Fryer, B. Wang, and H. Zheng. 2021. "Clusterin Secreted From Astrocyte Promotes Excitatory Synaptic Transmission and Ameliorates Alzheimer's Disease Neuropathology." *Molecular Neurodegeneration* 16, no. 1: 5. https://doi.org/10.1186/s13024-021-00426-7.

Clarke, L. E., S. A. Liddelow, C. Chakraborty, A. E. Munch, M. Heiman, and B. A. Barres. 2018. "Normal Aging Induces A1-Like Astrocyte Reactivity." *Proceedings of the National Academy of Sciences of the United States of America* 115, no. 8: E1896–E1905. https://doi.org/10.1073/pnas.1800165115.

Clavreul, S., L. Dumas, and K. Loulier. 2022. "Astrocyte Development in the Cerebral Cortex: Complexity of Their Origin, Genesis, and Maturation." *Frontiers in Neuroscience* 16: 916055. https://doi.org/10.3389/fnins.2022.916055.

Cordero-Llana, O., S. A. Scott, S. L. Maslen, et al. 2011. "Clusterin Secreted by Astrocytes Enhances Neuronal Differentiation From Human Neural Precursor Cells." *Cell Death and Differentiation* 18, no. 5: 907–913. https://doi.org/10.1038/cdd.2010.169.

Daneman, R., and A. Prat. 2015. "The Blood-Brain Barrier." *Cold Spring Harbor Perspectives in Biology* 7, no. 1: a020412. https://doi.org/10.1101/cshperspect.a020412.

Endogenous, H., Breast Cancer Collaborative, G, T. J. Key, P. N. Appleby, G. K. Reeves, and A. W. Roddam. 2010. "Insulin-Like Growth Factor 1 (IGF1), IGF Binding Protein 3 (IGFBP3), and Breast Cancer Risk: Pooled Individual Data Analysis of 17 Prospective Studies." *Lancet Oncology* 11, no. 6: 530–542. https://doi.org/10.1016/S1470-2045(10)70095-4.

Farhy-Tselnicker, I., and N. J. Allen. 2018. "Astrocytes, Neurons, Synapses: A Tripartite View on Cortical Circuit Development." *Neural Development* 13, no. 1: 7. https://doi.org/10.1186/s13064-018-0104-y.

Farhy-Tselnicker, I., M. M. Boisvert, H. Liu, et al. 2021. "Activity-Dependent Modulation of Synapse-Regulating Genes in Astrocytes." *eLife* 10: e70514. https://doi.org/10.7554/eLife.70514.

Ferris, H. A., R. J. Perry, G. V. Moreira, G. I. Shulman, J. D. Horton, and C. R. Kahn. 2017. "Loss of Astrocyte Cholesterol Synthesis Disrupts Neuronal Function and Alters Whole-Body Metabolism." *Proceedings of the National Academy of Sciences of the United States of America* 114, no. 5: 1189–1194. https://doi.org/10.1073/pnas.1620506114.

Filous, A. R., and J. Silver. 2016. "Targeting Astrocytes in CNS Injury and Disease: A Translational Research Approach." *Progress in Neurobiology* 144: 173–187. https://doi.org/10.1016/j.pneurobio.2016.03.009.

Flügge, G., C. Araya-Callis, E. Garea-Rodriguez, C. Stadelmann-Nessler, and E. Fuchs. 2014. "NDRG2 as a Marker Protein for Brain Astrocytes." *Cell and Tissue Research* 357, no. 1: 31–41. https://doi.org/10.1007/s00441-014-1837-5.

Fontanet, P. A., A. S. Rios, F. C. Alsina, G. Paratcha, and F. Ledda. 2018. "Pea3 Transcription Factors, Etv4 and Etv5, Are Required for Proper Hippocampal Dendrite Development and Plasticity." *Cerebral Cortex* 28, no. 1: 236–249. https://doi.org/10.1093/cercor/bhw372.

Freeman, M. R. 2010. "Specification and Morphogenesis of Astrocytes." *Science* 330, no. 6005: 774–778. https://doi.org/10.1126/science.1190928.

Fujita, H., H. Aoki, I. Ajioka, et al. 2014. "Detailed Expression Pattern of Aldolase C (Aldoc) in the Cerebellum, Retina and Other Areas of the CNS Studied in Aldoc-Venus Knock-In Mice." *PLoS One* 9, no. 1: e86679. https://doi.org/10.1371/journal.pone.0086679.

Futschik, M. E., and B. Carlisle. 2005. "Noise-Robust Soft Clustering of Gene Expression Time-Course Data." *Journal of Bioinformatics and Computational Biology* 3, no. 4: 965–988. https://doi.org/10.1142/s0219720005001375.

Guerreiro, R. J., J. Beck, J. R. Gibbs, et al. 2010. "Genetic Variability in CLU and Its Association With Alzheimer's Disease." *PLoS One* 5, no. 3: e9510. https://doi.org/10.1371/journal.pone.0009510.

Halassa, M. M., T. Fellin, H. Takano, J. H. Dong, and P. G. Haydon. 2007. "Synaptic Islands Defined by the Territory of a Single Astrocyte." *Journal of Neuroscience* 27, no. 24: 6473–6477. https://doi.org/10.1523/JNEUROSCI.1419-07.2007.

Hibino, H., A. Fujita, K. Iwai, M. Yamada, and Y. Kurachi. 2005. "Differential Assembly of Inwardly Rectifying K+ Channel Subunits, Kir4.1 and Kir5.1, in Brain Astrocytes." *FASEB Journal* 19, no. 5: A1161.

Hill, S. A., A. S. Blaeser, A. A. Coley, et al. 2019. "Sonic Hedgehog Signaling in Astrocytes Mediates Cell Type-Specific Synaptic Organization." *eLife* 8: e45545. https://doi.org/10.7554/eLife.45545.

Holt, L. M., R. D. Hernandez, N. L. Pacheco, B. Torres Ceja, M. Hossain, and M. L. Olsen. 2019. "Astrocyte Morphogenesis Is Dependent on BDNF Signaling via Astrocytic TrkB.T1." *eLife* 8: e44667. https://doi.org/10.7554/eLife.44667.

Holt, L. M., and M. L. Olsen. 2016. "Novel Applications of Magnetic Cell Sorting to Analyze Cell-Type Specific Gene and Protein Expression in the Central Nervous System." *PLoS One* 11, no. 2: e0150290. https://doi.org/10.1371/journal.pone.0150290.

Iadecola, C., and M. Nedergaard. 2007. "Glial Regulation of the Cerebral Microvasculature." *Nature Neuroscience* 10, no. 11: 1369–1376. https://doi.org/10.1038/nn2003.

Ishii, T., Y. Takanashi, K. Sugita, et al. 2017. "Endogenous Reactive Oxygen Species Cause Astrocyte Defects and Neuronal Dysfunctions in the Hippocampus: A New Model for Aging Brain." *Aging Cell* 16, no. 1: 39–51. https://doi.org/10.1111/acel.12523.

Itoh, M., S. Ide, S. Takashima, et al. 2007. "Methyl CpG-Binding Protein 2 (a Mutation of Which Causes Rett Syndrome) Directly Regulates Insulin-Like Growth Factor Binding Protein 3 in Mouse and Human Brains." *Journal of Neuropathology and Experimental Neurology* 66, no. 2: 117–123. https://doi.org/10.1097/nen.0b013e3180302078.

Jyothi, H. J., D. J. Vidyadhara, A. Mahadevan, et al. 2015. "Aging Causes Morphological Alterations in Astrocytes and Microglia in Human Substantia Nigra Pars Compacta." *Neurobiology of Aging* 36, no. 12: 3321–3333. https://doi.org/10.1016/j.neurobiolaging.2015.08.024.

Kanaan, N. M., J. H. Kordower, and T. J. Collier. 2010. "Age-Related Changes in Glial Cells of Dopamine Midbrain Subregions in Rhesus Monkeys." *Neurobiology of Aging* 31, no. 6: 937–952. https://doi.org/10.1016/j.neurobiolaging.2008.07.006.

Khakh, B. S., and M. V. Sofroniew. 2015. "Diversity of Astrocyte Functions and Phenotypes in Neural Circuits." *Nature Neuroscience* 18, no. 7: 942–952. https://doi.org/10.1038/nn.4043.

Kuiper, J. W., R. van Horssen, F. Oerlemans, et al. 2009. "Local ATP Generation by Brain-Type Creatine Kinase (CK-B) Facilitates Cell Motility." *PLoS One* 4, no. 3: e5030. https://doi.org/10.1371/journal.pone.0005030.

Kumar, L. M. E. F. 2007. "Mfuzz: A Software Package for Soft Clustering of Microarray Data." *Bioinformation* 2, no. 1: 5–7. https://doi.org/10.6026/97320630002005.

Lavialle, M., G. Aumann, E. Anlauf, F. Prols, M. Arpin, and A. Derouiche. 2011. "Structural Plasticity of Perisynaptic Astrocyte Processes Involves Ezrin and Metabotropic Glutamate Receptors." *Proceedings of the National Academy of Sciences of the United States of America* 108, no. 31: 12915–12919. https://doi.org/10.1073/pnas.1100957108.

Lee, J. A., B. Hall, J. Allsop, R. Alqarni, and S. P. Allen. 2021. "Lipid Metabolism in Astrocytic Structure and Function." *Seminars in Cell & Developmental Biology* 112: 123–136. https://doi.org/10.1016/j.semcdb.2020.07.017.

Liu, J., X. Feng, Y. Wang, X. Xia, and J. C. Zheng. 2022. "Astrocytes: GABAceptive and GABAergic Cells in the Brain." *Frontiers in Cellular Neuroscience* 16: 892497. https://doi.org/10.3389/fncel.2022.892497.

Luo, H., X. Q. Wu, M. Zhao, et al. 2017. "Expression of Vimentin and Glial Fibrillary Acidic Protein in Central Nervous System Development of Rats." *Asian Pacific Journal of Tropical Medicine* 10, no. 12: 1185–1189. https://doi.org/10.1016/j.apjtm.2017.10.027.

Mahmoud, S., M. Gharagozloo, C. Simard, and D. Gris. 2019. "Astrocytes Maintain Glutamate Homeostasis in the CNS by Controlling the Balance Between Glutamate Uptake and Release." *Cells* 8, no. 2: 184. https://doi.org/10.3390/cells8020184.

Matias, I., J. Morgado, and F. C. A. Gomes. 2019. "Astrocyte Heterogeneity: Impact to Brain Aging and Disease." *Frontiers in Aging Neuroscience* 11: 59. https://doi.org/10.3389/fnagi.2019.00059.

Matukumalli, S. R., R. Tangirala, and C. M. Rao. 2017. "Clusterin: Full-Length Protein and One of Its Chains Show Opposing Effects on Cellular Lipid Accumulation." *Scientific Reports* 7: 41235. https://doi.org/10.1038/srep41235.

Mazare, N., M. Oudart, J. Moulard, et al. 2020. "Local Translation in Perisynaptic Astrocytic Processes Is Specific and Changes After Fear Conditioning." *Cell Reports* 32, no. 8: 108076. https://doi.org/10.1016/j.celrep.2020.108076.

Miller, F. D., and A. S. Gauthier. 2007. "Timing Is Everything: Making Neurons Versus Glia in the Developing Cortex." *Neuron* 54, no. 3: 357–369. https://doi.org/10.1016/j.neuron.2007.04.019.

Molders, A., A. Koch, R. Menke, and N. Klocker. 2018. "Heterogeneity of the Astrocytic AMPA-Receptor Transcriptome." *Glia* 66, no. 12: 2604–2616. https://doi.org/10.1002/glia.23514.

Oberheim, N. A., X. Wang, S. Goldman, and M. Nedergaard. 2006. "Astrocytic Complexity Distinguishes the Human Brain." *Trends in Neurosciences* 29, no. 10: 547–553. https://doi.org/10.1016/j.tins.2006.08.004.

Obermeier, B., R. Daneman, and R. M. Ransohoff. 2013. "Development, Maintenance and Disruption of the Blood-Brain Barrier." *Nature Medicine* 19, no. 12: 1584–1596. https://doi.org/10.1038/nm.3407.

Ogata, K., and T. Kosaka. 2002. "Structural and Quantitative Analysis of Astrocytes in the Mouse Hippocampus." *Neuroscience* 113, no. 1: 221–233. https://doi.org/10.1016/s0306-4522(02)00041-6.

Olsen, R. W., and W. Sieghart. 2008. "International Union of Pharmacology.: LXX.: Subtypes of γ-Aminobutyric Acid Receptors:: Classification on the Basis of Subunit Composition, Pharmacology, and Function.: Update." *Pharmacological Reviews* 60, no. 3: 243–260. https://doi.org/10.1124/pr.108.00505.

Palmer, A. L., and S. S. Ousman. 2018. "Astrocytes and Aging." *Frontiers in Aging Neuroscience* 10: 337. https://doi.org/10.3389/fnagi.2018.00337.

Pessia, M., P. Imbrici, M. C. D'Adamo, L. Salvatore, and S. J. Tucker. 2001. "Differential pH Sensitivity of Kir4.1 and Kir4.2 Potassium Channels and Their Modulation by Heteropolymerisation With Kir5.1." *Journal of Physiology (London)* 532, no. 2: 359–367. https://doi.org/10.1111/j.1469-7793.2001.0359f.x.

Pfrieger, F. W., and N. Ungerer. 2011. "Cholesterol Metabolism in Neurons and Astrocytes." *Progress in Lipid Research* 50, no. 4: 357–371. https://doi.org/10.1016/j.plipres.2011.06.002.

Rusnakova, V., P. Honsa, D. Dzamba, A. Ståhlberg, M. Kubista, and M. Anderova. 2013. "Heterogeneity of Astrocytes: From Development to Injury-Single Cell Gene Expression." *PLoS One* 8, no. 8: e69734. https://doi.org/10.1371/journal.pone.0069734.

Sahni, V., Y. Itoh, S. J. Shnider, and J. D. Macklis. 2021. "Crim1 and Kelch-Like 14 Exert Complementary Dual-Directional Developmental Control Over Segmentally Specific Corticospinal Axon Projection Targeting." *Cell Reports* 37, no. 3: 109842. https://doi.org/10.1016/j.celrep.2021.109842.

Saili, K. S., T. J. Zurlinden, A. J. Schwab, et al. 2017. "Blood-Brain Barrier Development: Systems Modeling and Predictive Toxicology." *Birth Defects Research* 109, no. 20: 1680–1710. https://doi.org/10.1002/bdr2.1180.

Sakers, K., A. M. Lake, R. Khazanchi, et al. 2017. "Astrocytes Locally Translate Transcripts in Their Peripheral Processes." *Proceedings of the National Academy of Sciences of the United States of America* 114, no. 19: E3830–E3838. https://doi.org/10.1073/pnas.1617782114.

Sarthy, P. V., M. Fu, and J. Huang. 1991. "Developmental Expression of the Glial Fibrillary Acidic Protein (Gfap) Gene in the Mouse Retina." *Cellular and Molecular Neurobiology* 11, no. 6: 623–637. https://doi.org/10.1007/Bf00741450.

Shaltouki, A., J. Peng, Q. Liu, M. S. Rao, and X. Zeng. 2013. "Efficient Generation of Astrocytes From Human Pluripotent Stem Cells in Defined Conditions." *Stem Cells* 31, no. 5: 941–952. https://doi.org/10.1002/stem.1334.

Sofroniew, M. V., and H. V. Vinters. 2010. "Astrocytes: Biology and Pathology." *Acta Neuropathologica* 119, no. 1: 7–35. https://doi.org/10.1007/s00401-009-0619-8.

Soheili-Nezhad, S., O. Ibáñez-Solé, A. Izeta, J. H. J. Hoeijmakers, and T. Stoeger. 2024. "Time Is Ticking Faster for Long Genes in Aging." *Trends in Genetics* 40, no. 4: 299–312. https://doi.org/10.1016/j.tig.2024.01.009.

Soheili-Nezhad, S., R. J. van der Linden, M. O. Rikkert, E. Sprooten, and G. Poelmans. 2021. "Long Genes Are More Frequently Affected by Somatic Mutations and Show Reduced Expression in Alzheimer's Disease: Implications for Disease Etiology." *Alzheimers and Dementia* 17, no. 3: 489–499. https://doi.org/10.1002/alz.12211.

Swindell, W. R. 2011. "Metallothionein and the Biology of Aging." *Ageing Research Reviews* 10, no. 1: 132–145. https://doi.org/10.1016/j.arr.2010.09.007.

Tsai, H. H., H. Li, L. C. Fuentealba, et al. 2012. "Regional Astrocyte Allocation Regulates CNS Synaptogenesis and Repair." *Science* 337, no. 6092: 358–362. https://doi.org/10.1126/science.1222381.

Vasile, F., E. Dossi, and N. Rouach. 2017. "Human Astrocytes: Structure and Functions in the Healthy Brain." *Brain Structure & Function* 222, no. 5: 2017–2029. https://doi.org/10.1007/s00429-017-1383-5.

West, A. K., J. Hidalgo, D. Eddins, E. D. Levin, and M. Aschner. 2008. "Metallothionein in the Central Nervous System: Roles in Protection, Regeneration and Cognition." *Neurotoxicology* 29, no. 3: 489–503. https://doi.org/10.1016/j.neuro.2007.12.006.

Xiong, X. Y., Y. Tang, and Q. W. Yang. 2022. "Metabolic Changes Favor the Activity and Heterogeneity of Reactive Astrocytes." *Trends in Endocrinology and Metabolism* 33, no. 6: 390–400. https://doi.org/10.1016/j.tem.2022.03.001.

Yang, Z., and K. K. Wang. 2015. "Glial Fibrillary Acidic Protein: From Intermediate Filament Assembly and Gliosis to Neurobiomarker." *Trends in Neurosciences* 38, no. 6: 364–374. https://doi.org/10.1016/j.tins.2015.04.003.

Zarei-Kheirabadi, M., A. R. Vaccaro, V. Rahimi-Movaghar, S. Kiani, and H. Baharvand. 2020. "An Overview of Extrinsic and Intrinsic Mechanisms Involved in Astrocyte Development in the Central Nervous System." *Stem Cells and Development* 29, no. 5: 266–280. https://doi.org/10.1089/scd.2019.0189.

Zhou, B., Y. X. Zuo, and R. T. Jiang. 2019. "Astrocyte Morphology: Diversity, Plasticity, and Role in Neurological Diseases." *CNS Neuroscience & Therapeutics* 25, no. 6: 665–673. https://doi.org/10.1111/cns.13123.

Supporting Information

Additional supporting information can be found online in the Supporting Information section.